# KdotPsoft: Modelling and Simulation of Semiconductors and Device Physics

Sumanta Bose[a], Zhigan Song[a,b], W. J. Fan[a,c], D. H. Zhang[a]

[a] *School of Electrical and Electronic Engineering, Nanyang Technological University, Singapore*
[b] *SKLSM, Institute of Semiconductors, Chinese Academy of Sciences, China*
[c] *Corresponding author: ewjfan@ntu.edu.sg*

**Abstract**

We introduce a new platform called *KdotPsoft*, to model and simulate semiconductor quantum wells (QWs) and multiple QW (MQW) systems. It is suitable to design and study quantum cascaded lasers, vertical-cavity surface-emitting laser, etc in conjunction with experiment and fabrication. For fundamental physics and device physics applications, *KdotPsoft* is an ideal platform to model, simulate and study semiconductors QWs and MQW structures for fundamental physics and device physics applications. It can study MQW based structures such as quantum cascaded lasers (QCL), vertical-cavity surface-emitting laser (VCSEL), etc. *KdotPsoft* is based on the 16-band $\boldsymbol{k}\cdot\boldsymbol{p}$ perturbation theory model and it supports all conventional semiconductor materials, and also can works for dilute nitride and bismide doped semiconductors. As a demonstration, we will show a study an example case of lattice matched GaNBiAs/GaAs QWs and show its major results, such as the energy dispersion curves, optical gain spectra and electron-hole wavefunctions. At a larger scale, it can be used to comprehensively study the band lineups, energy dispersion relation, DOS, polarization-dependent transition matrix element strengths, optical gain/absorption spectra, spontaneous emission rate, radiative current density, electric field effects on the QW, etc. Advanced users may note that the development of the platform was done using Fortran and Python. We will strive to make *KdotPsoft* available as a independent platform or a Matlab toolbox in the future.

*Keywords:* $\boldsymbol{k}\cdot\boldsymbol{p}$ method, Electronic bandstructure, Optical properties, Semiconductor modelling and simulation

## 1. Introduction

Semiconductor quantum wells (QWs) are heterostructures in which a thin well layer of a lower bandgap material is sandwiched between two barrier layers of higher bandgap material [1, 2]. The well layer which is typically around 5–20 nm thick induces quantum confinement effect only in one dimension, whereas the movement in the other dimensions is unrestricted. This profoundly affects the density-of-states (DOS) and determines its electronic structure. Currently, they form an area of great scientific research interest, due to wide variety of potential applications in optoelectronic devices, such as quantum cascaded lasers (QCL), vertical-cavity surface-emitting laser (VCSEL), etc.

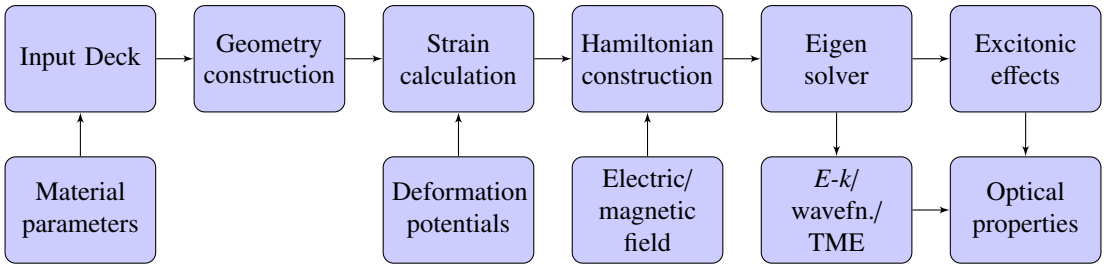


Figure 1: Flowchart showing the working flow of the *KdotPsoft* software. More info: kdotpsoft.com

In this work, we introduce a new platform, *KdotPsoft*, to simulate such semiconductor QW/ multiple QW (MQW) systems. Fig. 1 shows the flowchart summarizing the working flow of the *KdotPsoft* software. We have developed an

user-friendly GUI platform with built-in semiconductor material parameters. The input deck helps the user to design the QW/MWQ geometry from a choice of semiconductor materials and possible alloying. These material parameters could be manually altered by experienced users. After the QW geometry construction, the strain is calculated using material deformation potentials. As we will discuss in Sec. 2, we use the $\boldsymbol{k}\cdot\boldsymbol{p}$ model Hamiltonian, which is affected by the strain calculated in the previous step. In the $\boldsymbol{k}\cdot\boldsymbol{p}$ Hamiltonian construction, we can include optional electric field/ magnetic field terms if required to study those effects. Then Eigen solver is used to calculate the Eigen-energy values of the QW system. Additionally outputs include, DOS, the E-k dispersion energy bandstructure, electron-and-hole wavefunctions, band-lineup diagrams, polarization-dependent optical transition matrix, etc. The effect of excitonic recombination can also be considered for materials in which the excitonic binding energy is considerable. Finally, we can calculate the optical gain/absorption spectra, spontaneous emission rate, radiative current density, etc.

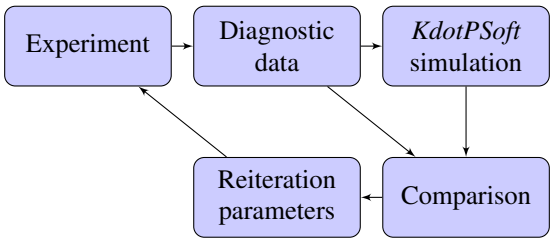


Figure 2: The setup of KdotPsoft software for experiments and fabrication.

Fig. 2 shows the setup of *KdotPsoft* software that can be used in both academia and industry to design experiments and predict optoelectronic characteristics for QCL, VCSEL experiments and fabrication. It can serve as a comparison tool between experimentally observed results and theoretically predicted results [3], and functions in a closed loop circuit as shown. It can be used to tune reiterations parameters for experiment and fabrication to reduce time and cost of production.

## 2. Theoretical Model

The core machinery of our *KdotPsoft* simulator is based on the $\boldsymbol{k}\cdot\boldsymbol{p}$ perturbation theory model. It takes into consideration the strain induced in the QW, which can modify the electronic states and degeneracy. Having accounted for these effects, it can calculate the energy eigenvalues for any QW combination composed of III-V, II-VI or group IV materials or alloys thereof. It is even capable of simulating the effect of dilute nitride and bismide doping in conventional III-V materials, which has been of increasing research interest recently [4]. *KdotPsoft* also gives the flexibility of simplifying the 10-band model to 8-band, 6-band and 4-band models by adjusting the nitrogen level, Kane matrix element, and spin-orbit (*so*) splitting energy respectively.

However, here we will describe the 16-band model, which is the superset of all lower band models and capable of incorporating even dilute nitride and dilute bismide semiconductor calculations. Earlier, Broderick *et al.* had proposed a 12- and 14-band Hamiltonian [5], but the 16-band model is more accurate, especially for the higher excited states of hole. The Kane's 8-band Hamiltonian has been extended using the band anticrossing (BAC) and valence BAC (VBAC) models, with the incorporation of two additional bands to address the local nitrogen resonant *s*-like states, and six more additional bands to address the local bismuth resonant *p*-like states considering the freedom of spin, including *so* coupling. The *KdotPsoft* 16-band Hamiltonian can be written in the form

$$H_{16\times16} = \begin{bmatrix} H_{2\times2} & H_{2\times8} & 0 \\ H_{8\times2} & H_{8\times8} & H_{8\times6} \\ 0 & H_{6\times8} & H_{6\times6} \end{bmatrix} \tag{1}$$

where $H_{8\times8}$ is the 8-band Hamiltonian containing both kinetic terms $H_k$ and strain terms $H_\varepsilon$, and given by [6]

$$H_{8\times8} = \begin{bmatrix} E^c & c.c. & c.c. & c.c. & c.c. & c.c. & c.c. & c.c. \\ 0 & E^c & c.c. & c.c. & c.c. & c.c. & c.c. & c.c. \\ \frac{1}{\sqrt{2}}P_- & 0 & P+Q & c.c. & c.c. & c.c. & c.c. & c.c. \\ -\sqrt{\frac{2}{3}}P_z & \frac{1}{\sqrt{6}}P_- & S^* & P-Q & c.c. & c.c. & c.c. & c.c. \\ -\frac{1}{\sqrt{6}}P_+ & -\sqrt{\frac{2}{3}}P_z & -R^* & 0 & P-Q & c.c. & c.c. & c.c. \\ 0 & -\frac{1}{\sqrt{2}}P_+ & 0 & -R^* & -S^* & P+Q & c.c. & c.c. \\ -\frac{1}{\sqrt{3}}P_z & -\frac{1}{\sqrt{3}}P_- & \frac{S^*}{\sqrt{2}} & -D & -\sqrt{\frac{3}{2}}S & \sqrt{2}R & P-\Delta & c.c. \\ -\frac{1}{\sqrt{3}}P_+ & \frac{1}{\sqrt{3}}P_z & -\sqrt{2}R^* & -\sqrt{\frac{3}{2}}S^* & D & \frac{S}{\sqrt{2}} & 0 & P-\Delta \end{bmatrix} \tag{2}$$

Detailed expressions of the $H_{8\times8}$ Hamiltonian terms are given in our previous work [6]. The $H_{2\times2}$ is the $s_N$-like localized N impurity Hamiltonian, while the $H_{6\times6}$ is the $p$-like localized Bi impurity Hamiltonian [2].

The $H_{8\times2}$ and $H_{6\times8}$ Hamiltonians account for the interaction of the $s_N$-like localized N impurity state and $p$-like localized Bi impurity state with the host material state, taking into consideration the BAC and VBAC coefficients [2].

We calculate the squared optical transition matrix element (TME) to calculate the optical gain, which is a measure of the momentum of transition strength between the hole and electron subband, and given by [7, 8]

$$\mathcal{P}_{cv,i} = \langle \Psi_{c,k} | \, e_i \cdot p \, | \Psi_{v,k} \rangle \quad , \quad i = x, y, z \tag{3}$$

where $\Psi_{c,k}$ and $\Psi_{v,k}$ are the real electron and hole wavefunctions respectively, and $\mathbf{p}$ is the momentum operator [9]. The reader is referred to ref. [9] for detailed expressions for the TMEs.

The following expression based on the density-matrix theory is used to calculate the optical gain spectra [10, 11].

$$G(E) = \left[1 - exp\left(\frac{E - \Delta F}{k_B T}\right)\right] \frac{\pi^2 c^2 \hbar^3}{n^2 E^2} R_{sp}(E) \tag{4}$$

$$R_{sp}(E) = \frac{ne^2 E}{\pi m_0^2 \varepsilon_0 \hbar^2 c^3} \sum_c \sum_v \int \int \frac{|\mathcal{P}_{cv}|^2}{4\pi^2 l} f_c f_v \times \frac{1}{\pi} \frac{\hbar/\tau}{(E_{eh} - E)^2 + (\hbar/\tau)^2} dk_x dk_y \tag{5}$$

where $R_{sp}(E)$ is the spontaneous emission rate. $f_c$ and $f_v$ are the Fermi-Dirac distributions for the electrons and holes in the CB and VB respectively that determine the Fermi factor [12].

## 3. Illustration and Discussion

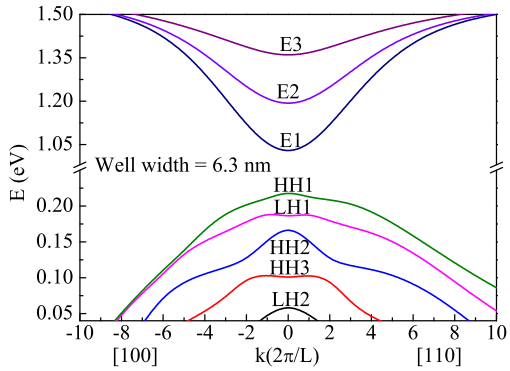


Figure 3: First 3 electron and first 5 hole energy dispersion curves of lattice matched GaNBiAs QWs of well width = 6.3 nm. E stands for electron, HH for heavy hole levels and LH for light hole levels. The photon emission energy is ~ 0.8 eV (1.55 $\mu$m). Reprinted from W. J. Fan, S. Bose, D. H. Zhang, "Electronic bandstructure and optical gain of lattice matched III-V dilute nitride bismide quantum wells for 1.55$\mu$m optical communication systems," Journal of Applied Physics 120 (9) (2016) 093111, with the permission of AIP Publishing.

As an illustration to demonstrate the working and application of the *KdotPsoft* software, we have chosen to study and show some major results for the case of $GaN_xBi_yAs_{1-x-y}$ semiconductor alloy QW pseudomorphically grown on GaAs. The bandgap of GaNBiAs depends on the compositions of N and Bi replacing the As from GaAs [2]. Here we choose to study the sample case of 6.3 nm thick $GaN_3Bi_{5.17}As_{91.83}$/GaAs QW. The reason of studying this composition is that the QW structure is a lattice matched QW, suitable for material growth, [2]. The emission wavelength is suitable for fiber optic laser diode applications. We found the energy dispersion curves for the first 3 electron and the first 5 holes subband states along the [100] and [110] wavevector direction for our QW case, which is shown in Fig. 3. *KdotPsoft* also enables us the determine the dominant hole type for each valence band, which is identified and indicated in Fig. 3. Here, the gap between to top of valence band (HH1) and bottom of conduction band (E1) is ~ 0.8 eV (1.55 $\mu$m), suitable for fiber optic laser diode applications.

The TE mode optical gain spectra of our lattice matched 6.3 nm GaNBiAs/GaAs QW case is shown in Fig. 4. The injection carrier density was varied from 2 to 8 $\times 10^{18}$ cm$^{-3}$, which determines the number of excitons available for recombination. The temperature considered was 300 K (RT). The intraband relaxation time $\tau$ was taken to be 0.1 ps. As the injection carrier density increases, the maximum gain increases due to greater excitonic recombinations, and there is a marginal blue shift in the emission peak position (called band filling effect).

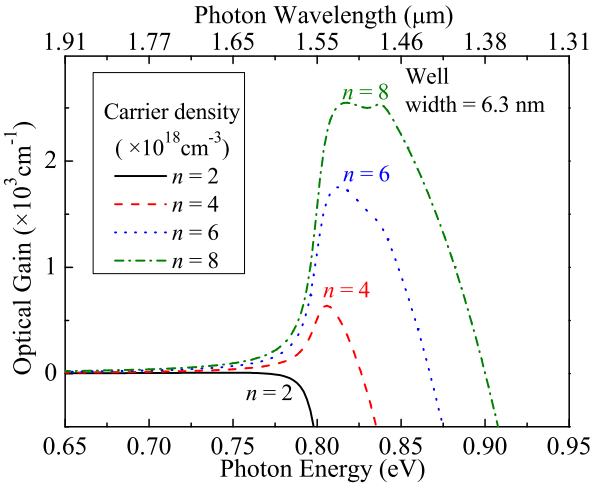


Figure 4: TE mode optical gain spectra of lattice matched GaNBiAs QWs at 300 K for well width = 6.3 nm and varying injection carrier density ($n$) = 2, 4, 6 and 8 $\times 10^{18}$ cm$^{-3}$. The peak emission position is ~ 0.8 eV (1.55 $\mu$m). Reprinted from W. J. Fan, S. Bose, D. H. Zhang, "Electronic bandstructure and optical gain of lattice matched III-V dilute nitride bismide quantum wells for 1.55$\mu$m optical communication systems," Journal of Applied Physics 120 (9) (2016) 093111, with the permission of AIP Publishing.

Fig. 5 shows the squared wavefunction (probability of finding electron of hole) of the first 3 electron and the first 5 hole energy levels at $\mathbf{k} = 0$ point for our lattice matched 6.3 nm GaNBiAs/GaAs QW case. The overlap between the HH1 and E1 facilitates the E1-HH1 excitonic recombination. A better overlap implies a higher TME value. The optical transition rule is followed for the transitions, which also depends on the extent of wavefunction overlap.

## 4. Summary and Conclusion

*KdotPsoft* is an ideal platform to model, simulate and study semiconductors quantum well (QW) and multiple QW structures for fundamental physics and device physics applications. It can study MQW based structures such as quantum cascaded lasers (QCL), vertical-cavity surface-emitting laser (VCSEL), etc. *KdotPsoft* is based on the 16-band $\boldsymbol{k}\cdot\boldsymbol{p}$ perturbation theory model and it supports all conventional semiconductor materials, and also can works for dilute nitride and bismide doped semiconductors. As a demonstration, we have studied and shown some major results for 6.3 nm thick lattice matched GaNBiAs/GaAs QWs, such as – the energy dispersion curves, optical gain spectra and electron-hole wavefunctions. At a larger scale, it can be used to comprehensively study the band lineups, energy dispersion relation, DOS, polarization-dependent transition matrix element strengths, optical gain/absorption spectra, spontaneous emission rate, radiative current density, electric field effects on the QW, etc.

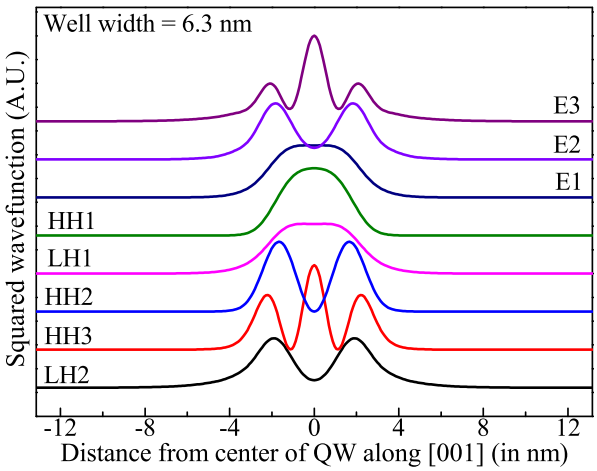


Figure 5: First 3 electron and first 5 hole squared wavefunctions at $\mathbf{k} = 0$ point for GaNBiAs QWs of well width = 6.3 nm vs. distance from the center plane of QW along the [001] direction. E stands for electron, HH for heavy hole levels and LH for light hole levels. Reprinted from W. J. Fan, S. Bose, D. H. Zhang, "Electronic bandstructure and optical gain of lattice matched III-V dilute nitride bismide quantum wells for 1.55$\mu$m optical communication systems," Journal of Applied Physics 120 (9) (2016) 093111, with the permission of AIP Publishing.

## 5. References


[1] C. A. Broderick, P. E. Harnedy, E. P. OReilly, Theory of the electronic and optical properties of dilute bismide quantum well lasers, IEEE J. Sel. Top. Quantum Electron. 21 (6) (2015) 287–299.
URL http://dx.doi.org/10.1109/JSTQE.2015.2448652

[2] W. J. Fan, S. Bose, D. H. Zhang, Electronic bandstructure and optical gain of lattice matched III-V dilute nitride bismide quantum wells for 1.55$\mu$m optical communication systems, Journal of Applied Physics 120 (9) (2016) 093111. doi:10.1063/1.4962214.
URL http://dx.doi.org/10.1063/1.4962214

[3] S. Bose, S. Delikanli, A. Yeltik, M. Sharma, O. Erdem, C. Dang, W. Fan, D. H. Zhang, H. V. Demir, Anomalous spectral characteristics of ultrathin sub-nm colloidal cdse nanoplatelets, in: Conference on Lasers and Electro-Optics, Optical Society of America, 2017, p. SM1K.2. doi:10.1364/CLEO_SI.2017.SM1K.2.
URL http://www.osapublishing.org/abstract.cfm?URI=CLEO_SI-2017-SM1K.2

[4] Z. Song, S. Bose, W. Fan, D. H. Zhang, Y. Y. Zhang, S. S. Li, Quantum spin Hall effect and topological phase transition in $InN_xBi_ySb_{1-x-y}$/InSb quantum wells, New Journal of Physics 19 (7) 073031. doi:10.1088/1367-2630/aa795c.

[5] C. A. Broderick, M. Usman, E. P. O'Reilly, Derivation of 12- and 14-band $\boldsymbol{k}\cdot\boldsymbol{p}$ hamiltonians for dilute bismide and bismide-nitride semiconductors, Semicon. Sci. and Tech. 28 (12) (2013) 125025.
URL http://dx.doi.org/10.1088/0268-1242/28/12/125025

[6] W. J. Fan, Orientation dependence of electronic structure and optical gain of (11N)-oriented III-V-N quantum wells, J. Appl. Phys. 113 (8) (2013) 083102.
URL http://dx.doi.org/10.1063/1.4793279

[7] S. Bose, Z. Song, W. J. Fan, D. H. Zhang, Effect of Lateral Size and Thickness on the Electronic Structure and Optical Properties of Quasi Two-dimensional CdSe and CdS Nanoplatelets, Journal of Applied Physics 119 (14) (2016) 143107. doi:10.1063/1.4945993.
URL http://dx.doi.org/10.1063/1.4945993

[8] Z.-G. Song, S. Bose, W.-J. Fan, S.-S. Li, Electronic band structure and optical gain of $GaN_xBi_yAs_{1-x-y}$/GaAs pyramidal quantum dots, Journal of Applied Physics 119 (14) (2016) 143103. doi:10.1063/1.4945700.
URL http://dx.doi.org/10.1063/1.4945700

[9] W. J. Fan, M. F. Li, T. C. Chong, J. B. Xia, Valence hole subbands and optical gain spectra of GaN/$Ga_{1-x}Al_xN$ strained quantum wells, J. Appl. Phys. 80 (6) (1996) 3471. doi:10.1063/1.363217.

[10] J. Minch, S. H. Park, T. Keating, S. L. Chuang, Theory and experiment of $In_{1-x}Ga_xAs_yP_{1-y}$ and $In_{1-x-y}Ga_xAl_yAs$ long-wavelength strained quantum-well lasers, IEEE J. Quant. Electron. 35 (5) (1999) 771–782. doi:10.1109/3.760325.

[11] S. T. Ng, W. J. Fan, Y. X. Dang, S. F. Yoon, Comparison of electronic band structure and optical transparency conditions of $In_xGa_{1-x}As_{1-y}N_y$/GaAs quantum wells calculated by 10-band, 8-band, and 6-band k·p models, Phys. Rev. B 72 (2005) 115341. doi:10.1103/PhysRevB.72.115341.
URL http://link.aps.org/doi/10.1103/PhysRevB.72.115341

[12] S. Bose, S. Shendre, Z. Song, V. K. Sharma, D. H. Zhang, C. Dang, W. Fan, H. V. Demir, Temperature-dependent optoelectronic properties of quasi-2D colloidal cadmium selenide nanoplatelets, Nanoscale 9 (2017) 6595–6605. doi:10.1039/C7NR00163K.
URL http://dx.doi.org/10.1039/C7NR00163K